Damanhour Journal of Veterinary Sciences 6 (2), (2021) 1-6

Damanhour Journal of Veterinary Sciences

Journal homepage: https://djvs.journals.ekb.eg/

Comparative pilot study of radiography and computed tomography for the thorax of Shirazi cat

Alaa Ibrahim[1], Ahmed Nomir[1], Doaa Emara[2], Ashraf El Sharaby[1,*]

[1]Department of Anatomy and Embryology, Faculty of Veterinary Medicine, Damanhour University, Damanhour, Egypt.

[2]Department of Radiology, Faculty of Medicine, Alexandria University, Alexandria, Egypt.

A B S T R A C T

The purpose of this pilot study was to validate the use of computed tomography (CT) for documenting the anatomy of the thorax of Shirazi cats. We used 3 clinically normal adult Shirazi cats, which were screened for radiographic and CT views and then used for reference gross dissection. Thorax CT scan displayed through hundreds of views the thoracic cage, trachea, bronchi, lungs, heart, vessels, mediastinum, and pleural cavity not only on sagittal and coronal planes but also – and exceptionally – on a transverse plane providing precise and unique information that was unobtainable with radiographs. CT scan also provided soft and lung windows, both of which enabled proficient tracing of the position, shape, and size of all the thoracic structures. The obtained radiographic and CT findings in the thorax of the investigated cats have been compared, and several anticipated parameters of the two screening techniques were evaluated and discussed. Our results indicated that radiographic scans remain a fast and easy start point for thoracic examination enough for an emergency diagnosis, whereas CT images are superior to identify anatomical structures and subsequent clinical interpretation of the feline thoracic affections. Anatomical reference study of the thoracic CT images is proposed for all screening levels of Shirazi cat.

Keywords: X-ray, CT, Thorax, Cat, Anatomy

1. Introduction

Veterinary imaging includes modalities such as radiographs (x-rays), ultrasound microscopy, computed tomography (CT scans) and magnetic resonance imaging (MRI). The feline thorax may be easily examined radiographically (Farrow et al., 1994), but mediastinal structures are superimposed on radiographs; in particular, the cranial part of mediastinum is not individually identifiable (Suter 1984, Thrall 1994). Conventional radiology film continues to be the mainstay of thoracic imaging; however, the obtained views are limited to lateral and dorsoventral and/ or ventro-dorsal projection (Hayward et al., 2004; Johnson et al., 2008; Guglielmini and Diana, 2015). Since thorax CT has been introduced in veterinary medicine (Burk, 1991), it becomes widely accepted as a specialized imaging modality. It provides radiography-based thin cross-sectional images without disturbing internal structures (Rycke et al., 2004 and Irausquin et al., 2008), and eliminates super imposition of structures and harmony improve quality resolution (Al-Akraa et al., 2015). It allows better distinction among specific tissue densities in the thorax and displays the lungs, mediastinum, pleural cavity, and chest wall, and provides unique information that is unobtainable with conventional radiographs (Chen et al., 1992, Hathcock and Stickle 1993, Henninger, 2003). Reports of CT-based anatomy make interpretation of thoracic scans easier, thus providing increased diagnostic information and allowing more specific therapy (Schwarz and Tidwell 1999).

*Corresponding author

E-mail: elsharaby@yahoo.com

Address: Department of Anatomy and Embryology, Faculty of Veterinary Medicine, Damanhour University, Damanhour, Egypt..

However, the frequency of the use of CT for thoracic imaging in the reported literature is lower than for imaging other regions. To our knowledge, clinically relevant CT reports on the anatomy of the thorax of cat are few (Samii et al., 1998; Shojaei et al., 2003; Vladova et al., 2005), which were based a comparison of the obtained CT images only with normal cross- anatomical sections. Skillful person aware with information of gross anatomy is required to locate the organs on CT image (Al-Akraa et al., 2015), and long-term benefits for the thoracic CT have yet to be realized or determined and there are still no comparable anatomy reports for lateral, dorsoventral or ventrodorsal radiographs. Therefore, the present study was performed to identify anatomic structures of CT images of the Shirazi cat thoracic region, with particular emphasis on their comparison with radiographs for use by veterinary radiologists and clinicians.

2. Materials and Method

2.1. Animal preparation

Three clinically normal adult Shirazi cats of 2.5 to 3 years old weighing 3 to 5 kg were used in the present study. Prior to the conduction of our experiments, the cats were sedated with intravenous injection of xylazine (1 mg/kg) and atropine 0.05 mg/kg) for induction and ketamine (5-10 mg/kg) for the maintenance of general anesthesia.

Radiography (X-ray imaging):

According to Reed and Axam (2017), the cats were properly positioned in sternal recumbency on the scanning table with their forelimbs in extension to collect dorsoventral radiographic views. Then, cats were positioned on their lateral aspects for screening the right and left lateral sides. The radiographic views were made by use of Toshiba 500 mA and FCR Prima T2 X-ray device. Hard copies of the dorsoventral and lateral radiographic views were printed out on x-ray films and soft copies were also obtained for offline surveying the thorax.

2.2. Computed tomography (CT)

Right and left lateral radiographic views of the thorax of each cat were investigated for normal anatomical morphology prior to the onset of CT examination. Cats were positioned in sternal recumbency on the scanning table with their forelimbs in extension. Tomograms were made almost perpendicular to the longitudinal axis of the thorax from the thoracic inlet to diaphragm to get transverse and coronal slices, and then changed parallel to longitudinal axis to get sagittal slices. Contiguous images were obtained using a general diagnostic CT system (Toshiba xvid; scanning conditions: 80 kV, 171 mA., 4 second) set for soft window. The slice thickness was 1.3-mm for transverse views and 2.22-mm for sagittal and coronal views. Lung window was obtained from the CT system by changing the settings (window width, 1,000 Hounsfield units; window level, −690 Hounsfield units according to De Rycke et al. (2005). The cats were then photographed for 3D images of thoracic skeleton on the same CT system. For documentation, the CT scanned images were printed as hard copies and digital workstation images were saved on a hard drive for offline investigation using RadiAnt DICOM Viewer software; version 2020.2.3. Nomenclature of the relevant structures and landmarks of the thorax were identified and labelled on CT images according to Shojaei et al. (2003).

2.3. Radiography and CT evaluation

A custom-designed list of the anticipated parameters for both radiography and CT was prepared, filled out (Table 1) and then evaluated and discussed.

2.4. Dissection of animals

After screening examinations, the cats were euthanized, fixed by 10% formalin, and then dissected out and used as reference of the thoracic anatomic structures.

3. Results

3.1. Radiography (X-Ray)

The thoracic cage of the adult Shirazi cat was bounded dorsally by 13 thoracic vertebrae, laterally by 13 pairs of ribs and ventrally by the sternum (Fig. 1). All the bones and cartilages presented high contrast compared to the thoracic visceral contents. We outlined the area of attachment of the diaphragm, location of the esophagus, heart, and great vessels as well as the right and left lungs and their extension limits. The cranial mediastinum may be widened and the contribution of pericardial fat to the overall shape of the cardiac silhouette may not be discernable. As presented in lateral radiographs, the heart was the largest organ of soft tissue opacity within the thorax and located in the middle mediastinum traversing from approximately the fourth to the sixth intercostal space (Fig. 2A). The base was the wider and most dorsal part of the heart, while the apex is narrower and sloping caudally and ventrally. In dorsoventral radiographs, most parts of the heart were located left to the midline (Fig. 2B). The cranial and caudal borders of the cardiac outline define the cranial and caudal edge of the right and left ventricle, respectively. We could not observe the internal chambers of the heart on all thoracic radiographic projections, meanwhile the great vessels specially the aorta, brachiocephalic trunk and caudal vena cava were clearly observed.

3.2. Computed tomography (CT)

We obtained excellent soft and lung window images of the thorax and soft tissue architecture. and collected thin multi-slice and contiguous views at transverse (Fig. 2 and 3), sagittal (Fig. 4 and 5) and coronal (Fig. 6) levels of the cat. Thorax average number of transverse slices was about 112 out of 428 total scanned slices for the whole body, for sagittal slices was 42 out of 51 total scanned slices, and for coronal slices about 44 out of 49 total scanned slices for the whole body. Soft window views (Fig. 2, 4, 6A) and lung window views (Fig. 3, 5, 6B) showed different levels of tissue density. A higher density was constantly shown for the thoracic cage, which was composed dorsally of 13 thoracic vertebrae (ThV), laterally of 13 pairs ribs (Ri) and ventrally of 8 sternebrae (S). Mediastinum was observed as low dense sagittal partition alongside the midline of the thorax. Cranial mediastinum (Mcr) extended from the thoracic inlet to 3rd intercostal space (Fig. 2A and 3A), middle mediastinum (Mmi) between 4th and 6th intercostal spaces (2B and 6B) and caudal mediastinum (Mcd) continued till the diaphragm (D) (Fig. 3B). In soft window views, the right (RL) and left (LL) lungs as well as the trachea (Tr) and esophagus (Es) were represented by consolidated black areas. In lung window views, lobes of the lungs remained black except the intralobar vessels, which became readily visible. We also observed the right and left bronchi (RB and LB, respectively) with the associated pulmonary arteries and veins (Fig. 3B). The heart and great vessels were visible with appreciable density in both soft and lung windows. The heart was located between the 4th and 6th intercostal spaces where its longitudinal axis was parallel to the sternum with a cranially oriented base (Hb) and a rounded caudal apex (Ha). Chambers of the heart and great vessels of the thorax were clearly observed including the aortic arch (Aoa); thoracic aorta (Ao); pulmonary trunk and arteries (Pt) left subclavian artery (LsA); right brachiocephalic artery (RBa) as well as caudal vena cava (CVC).

3.3. 3D imaging

The relationship between various organs and structures was easily visualized by the used CT screening system, which enabled a sophisticated 3D reconstructions of the thoracic cage and its contents specially the heart (Fig. 7).

Comparison of radiograph and CT imaging:

Table 1 illustrates radiographic and CT imaging of the investigated Shirazi cats (n=3).

Discussion:

Our intent in the present study was to mainly to evaluate the screening views obtained from conventional radiography with the viewing opportunities available in the CT system. Similar to the findings of Suter (1984); Farrow et al. (1994); Thrall (1994); Hayward et al., (2004); Johnson et al. (2008); Guglielmini and Diana (2015), we found radiographs proved a substantial clarification of the components of thoracic cage but fairly outlined the topography of organs and vascular structures. However, superimposition of the heart and the lungs was observed over thoracic structures especially those in the mediastinum. On the other hand, thin slices of the CT at sagittal, transverse, and coronal planes provided clear, unobstructed images and improved demonstration of individual structures of the thorax. All anatomical structures of the thoracic cavity were clearly identified and were very similar to those denoted by Samii et al. (1998) and Shojaei et al. (2003).

3.4. Thorax Positioning

The goal of positioning the patient for any radiograph is to place the animal so that the anatomy is accurately represented. Knowledge of positioning and anatomy is crucial to producing a radiograph that will afford the clinician the greatest chance of making an accurate diagnosis (Matt, 2014). The standard views for radiographic evaluation of the thorax are the lateral view and dorsoventral (DV) or ventrodorsal (VD) projection (Guglielmini and Diana, 2015). These radiographs should be centered on the 5th intercostal space to include the heart, entire lung field and the surrounding ribs (Reed and Axam, 2017). The canine heart is less affected by chest conformation when the patient is placed in the DV position (Holmes et al., 1985). The vessels in the caudal lung lobes, which are important in evaluating heart disease, are better magnified in the DV position in both dogs and cats (Carlisle and Thrall, 1982). In the present study, the collected radiographs offered only one shot per each posture, meanwhile CT scans provided hundreds of high contrast slices with detailed information at all levels including the transverse planes which was not obtained by radiography.

Previous CT anatomy relevant studies in the cat were constantly based on the transverse views obtained by the CT and relate them with transverse anatomical sections (Samii et al., 1998; Shojaei et al., 2003; Vladova et al., 2005; Pazvant et al., 2012; A l-Akraa et al., 2015; Masseau and Reinero, 2019). One of the new findings in this study is the availability of thin and multi-slice sagittal and coronal projections of the thorax, which undoubtedly extended the advantage of CT for clear visualization of anatomic features and individual differences. We were fortunate to utilize this data series to outline the mediastinum and its anatomic relations with the trachea, esophagus, lungs, heart, cranial and caudal vena cavae and other structures. Further anatomical reference studies are needed to clarify all screening levels of the CT.

3.5. Radiography Contrast versus CT windows

Technique settings with proper radiographic density and contrast are crucial, and without contrast, it would not be possible to view discrete anatomical structures. In the present study, this was limited for radiographs not for the CT, which provided soft and lung windows. The opportunity of the CT which enabled us for proficient tracing of position, shape, and size of all thoracic contents as well as 3D reconstructions of thoracic structures. In agreement with Thrall (2013), the results of our evaluation list in Table 1 confirmed that CT imaging offer superior imaging qualities over conventional radiography. Meanwhile radiographs represent two dimensional or flat structures, projections of the thorax that had three-dimensional structures, tissues were easily examined with CT in thin slices. This facility eliminated superimposition and thereby one easily identifies thoracic organs and structures, which was extremely limited in conventional radiographs. Moreover, we were able to reformate the obtained CT volume image workstation in the favorable imaging plane, or as 3D reconstruction.

4. Conclusion

We conclude that conventional radiography is inconclusive or insufficient to provide different levels of tissue density and more detailed images at all planes than do the CT, which is the technique of choice for clear visualization of anatomic features, individual differences, and the diagnosis of feline thorax pathology.

Conflict of interest statement

No conflicts of interest.

Funding
The authors declared that they received no financial support for their research and/or authorship of this article.

5. References

Al-Akraa, A., Ghanem, M., El-gezery, M., 2015. Hepatosonography and Computed Tomography in Feline. Benha Vet Med J., 28, 1: 33-42.
Burk, R. L. (1991): Computed tomography of thoracic diseases in dogs. J Am Vet Med A; 199, 617-621.
Carlisle C.H., Thrall D.E., 1982. A comparison of normal feline thoracic radiographs made in dorsal versus ventral recumbency. Veterinary Radiology. 1982; 23 (1): 3-9.
Chen Q., Klein J. S., Gamsu G. and Webb W.R., 1992. High-resolution computed tomography of the mammalian lung. Am J Vet Res.; 53, 1218-1224.
De Rycke, L. M., Gielen, I. M., Simoens, P. J. and van Bree, H., 2005. Computed tomography and cross-sectional anatomy of the thorax in clinically normal dogs. American Journal of Veterinary Research, 66, (3): 512–524.
Farrow, C. S., Green, R. and Shively, M., 1994. Radiology of the cat. pp 45-130. Mosby, St. Louis.
Farrow C.S., Green R., Shively M. The thorax. In: Farrow CS, Green R, Shively M, editors. Radiology of the cat. St Louis: Mosby; 1994. p. 45-130.
Guglielmini C. and Diana A., 2015. Thoracic radiography in the cat: Identification of cardiomegaly and congestive heart failure. J Vet Cardiology; 17, S87-S101.
Hamlin RL, Smetzer DL, Smith CR., 1963. Radiographic anatomy of the normal cat heart. J Am Vet Med Assoc; 146: 957-961.
Hathcock, J. T. and Stickle, R. L., 1993. Principles and concepts of computed tomography. Veterinary Clinics of North America: Small Animal Practice 23, 399-416.
Hayward N.J., Baines S.J., Baines E.A., Herrtage ME., 2004. The radiographic appearance of the pulmonary vasculature in the cat. Vet Radiol Ultrasound; 45: 501-504.
Henninger W., 2003.: Use of computed tomography in the diseased feline thorax. J Small Anim Pract; 44 (2) :56-64. doi: 10.1111/j.1748-5827.2003.tb00121.x.
Holmes R.A., Smith F.G., Lewis R.E., Kern D.M., 1985. The effects of rotation on the radiographic appearance of the canine cardiac silhouette in dorsal recumbency. Veterinary Radiology and Ultrasound; 26 (3): 98-101.
Irausquin R.A., Scavelli T.D., Corti L., Stefanacci J.D. DeMarco J., Flood S., and Rohrbach B.W. 2008. Comparative evaluation of the liver in dogs with a splenic mass by using ultrasonography and contrast-enhanced computed tomography. Can Vet J; 49 (1): 46–52.
Johnson V., Hansson K., Maı W., Dukes-McEwan J., Lester N., Schwarz T., Chapman P., Morandi F. (2008): The heart and major vessels. In: Schwarz T, Johnson V, editors.
Kazemi-Darabadi, S. Akbari G., Ebrahimi E., Zangisheh M. (2018): Computed tomographic anatomy and topography of the lower respiratory system of the southern white-breasted hedgehog (erinaceus concolor). Iranian J of Veterinary Surgery; 13: 2, 29, Pages 26-33.
Masseau I. and Reinero C.R., 2019. Thoracic computed tomographic interpretation for clinicians to aid in the diagnosis of dogs and cats with respiratory disease. Vet J; 253:
Prather, A. B., Berry, C. R and Thrall, D. E., 2005. Use of radiography in combination with computed tomography for the assessment of noncardiac thoracic disease in the dog and cat. Vet Radiol Ultrasound, 46 (2), 114–121. Doi:10.1111/j.1740-8261.2005.00023.x
Pazvant G., Gezer İnce N., Bacinoğlu D., Bakirel, U., 2012. Examination of morphometry of feline thoracic aorta with computed tomography. Turk. J. Vet. Anim. Sci.; 36 (6): 698-704. doi:10.3906/vet-1107-40.
Reed A. and Axam T., 2017. Diagnostic imaging for technicians: Positioning and technique for thoracic and abdominal Radiographs. Veterinary Nursing Education, Oct/Nov: 40-47.
Rivero, M.A., Ramı´rez, J.A., Va´zquez, J. M., F. Gil, Ramı´rez, G. and Arencibia, A. 2005. Normal anatomical imaging of the thorax in three dogs: computed tomography and macroscopic cross sections with vascular injection. Anat. Histol. Embryol. 34: 215–219.
Rycke L.M., Gielen, I.M., Paul, J. and Bree H., 2005. Computed tomography and cross-sectional anatomy of the thorax in clinically normal dogs. AJVR: 66(3): 524-512.
Samii V.F., Biller D.S., and Koblik, P.D., 1998. Normal cross-sectional anatomy of the feline thorax and abdomen: comparison of computed tomography and cadaver anatomy. Vet Radiol and Ultrasound, 39, 6: 504-511. doi.org/10.1111/j.1740-8261.1998.tb01640.x
Thrall D. E., 2013. Textbook of Veterinary Diagnostic Radiology—E-Book. Elsevier Health Sciences.
Vladova, D., P. Georgiev, Y. Toneva, H. Georgiev, D. Sivrev and M. Stefanov (2005): Comparative anatomy of the feline heart in topographic, computer tomographic and echographic cross-sections. Trakia Journal of Sciences, Vol. 3, Suppl., 2, pp. 30-33.
Wright M., 2014. Treat Radiation with Respect, Not Anxiety. Veterinary Practice News. Updated August 8, 2010. Accessed June 1, 2014.

Table 1 illustrates radiographic and CT imaging of the investigated Shirazi cats (n=3).

Basis for comparison	Radiographs (X-rays)	Computed tomography CT
Sedation	Cats were not sedated.	Cats must be sedated.
Posturing of cat	Change according to required plane	Not changed on scanner.
Density	Mostly bones.	Bones, organs, and vessels.
Imaging planes (Sides)	Dorsoventral (DV), ventrodorsal (VD) and lateromedial.	Transverse, sagittal and coronal.
Imaging time	5 – 10 minutes.	20 – 30 minutes.
Side /side	Identically similar shotting.	3D.
Image Dimensions	Consolidated 2D.	Multi-slice 3D.
View thickness	Whole side thickness.	Thin slice.
Delivered image (s)	One per shot.	Multi-slice and contiguous (hundreds or more per plane)
Superimposition of structures	Extensive causing opacity.	Thin slices eliminate superimposition.
Structural anatomic relationship	Weakly supported.	Highly effective.
3D reconstruction	Available.	Not available.
Reformatting digital images	Not supported.	Provided high-quality images.

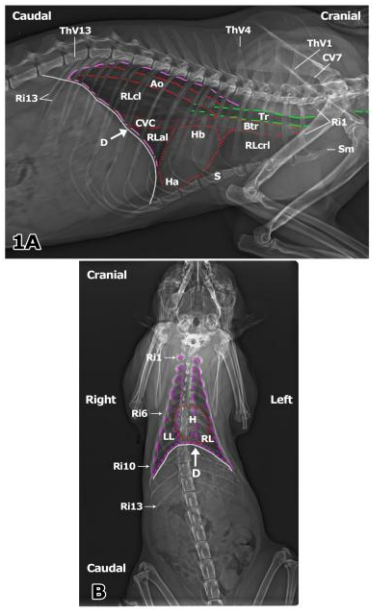

Figure 1: Lateral (1A) and dorsoventral (1B) radiographs of the thorax of a healthy 2.5-year-old Shirazi cat showing the thoracic cage, which was bounded dorsally by 13 thoracic vertebrae (ThV1-13), laterally by 13

pairs of ribs (Ri1-13) and ventrally by the sternum (S). Thoracic radiographs clearly presented the lobes of right lung; cranial (RLcrl), accessory (RLal) and caudal lobe (RLcl); the heart base and apex (Hb and Ha, respectively) and the great vessels including the aorta (Ao), brachiocephalic trunk (Btr) and caudal vena cava (CVC) as well as the trachea (Tr). attachment of first rib (Ri1) to last cervical vertebra (CV7). Superimposition of thoracic structures i.e., bones of the thoracic cage, right lung masking the left one, and the trachea masking the esophagus and surrounding vessels. Arrowheads show the continuous white line illustrate the area of attachment of diaphragm; red dotted lines outline the heart and great vessels; dashed pink lines outline the extension limits of the right and left lungs.

Figure 2: CT soft windows of the selected transverse slices of a healthy 3-year-old Shirazi cat showing the architecture of the thorax and its contents. The selected slice No. 144 (Fig. 2A) was scanned about the level of the 2nd thoracic vertebra i.e., cranial mediastinum, meanwhile the slice No. 178 (Fig. 2B) was scanned about the level of the 5th thoracic vertebra i.e middle mediastinum. Notice the higher density of the components of thoracic cage, which was formed dorsally by the 2nd/ 5th thoracic vertebra (ThV2/ 5), laterally by the 3rd / 6th rib (Ri3/ 6) and ventrally by the sternum (S). The trachea (Tr), and right (RL) and left (LL) lungs appeared as black areas meanwhile other structures within the mediastinum as the heart (RV and LV), aorta (Ao), pulmonary trunk (Pt), and other structures were gray but clearly discernible. Thoracic aorta (Ao) was found dorsal to the tracheal bifurcation (TrB).

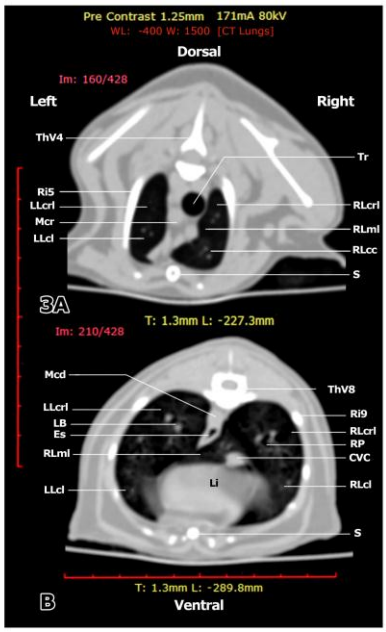

Figure 3: CT lung windows of the selected transverse slices of a healthy 3-year-old Shirazi cat showing architecture of the thorax with a higher density of the lungs, trachea (Tr), left bronchus (LB) and intralobar vessels versus the other components of the thorax. The selected slice No. 160 (Fig. 6A) was scanned about the level of the 4th thoracic vertebra (ThV4); middle mediastinum, meanwhile the selected slice No. 210 (Fig. 6B) was scanned about the level of 8th thoracic vertebra (ThV8) i.e. caudal mediastinum. The trachea (Tr) was clearly visible as a black circle in the cranial mediastinum (M) right to the midline. In Fig. 6B, there lobes of right lung; cranial (RLcrl), middle (RLml), and caudal (RLcl) and the two lobes of left lung; cranial (LLcrl) and caudal (LLcl) were clearly observed. Emergence of the caudal vena cava (CVC) from the liver (Li) through the diaphragm (D) as well as the right (RB) and left (LB) bronchi with their arteries and veins.

Figure 4: CT bone window of the sagittal slices of a healthy 3-year-old Shirazi cat showing the architecture of the thorax and its contents. The selected slices were about the midline of the scanned cat where 2A represent the slice No. 21 which was right to the midline; slice No. 24 was about the midline while slice No. 26 was left to the midline. Notice the higher density of the components of thoracic cage; thoracic vertebrae (ThV 1-13), ribs (Ri 1-13) and the sternum (S). The heart was located between the 4th and 6th ribs where its longitudinal axis was parallel to the sternum with a cranially oriented base (Hb) and a rounded caudal apex (Ha). Great vessels of the thorax were clearly observed including the aortic arch (Aoa); thoracic aorta (Ao); left subclavian artery (LsA); right brachiocephalic artery (RBa) and caudal vena cava (CVC). One can hardly distinguish the lobes of the two lungs from the esophagus (Es) or trachea (Tr) as they all were represented by black areas.

Fig 5: CT lung window of the sagittal slices of a healthy 3-year-old Shirazi cat showing architecture of the thorax with a higher density of the lungs, trachea (Tr) and pulmonary artery (Pa) and intralobar vessels versus the other components of the thorax. The selected slices were about the midline of the scanned cat where 3A represented the slice No. 21, which was right to the midline; slice No. 26 was at the midline while slice No. 30 was left to the midline. In Fig. 3C, the caudal vena cava (CVC) emerged from the diaphragm (D) into the thoracic cavity and coursed cranial wards between the caudal lobe (RLcl) and accessory (RLal) lobe of the right lung to open into the right atrium.

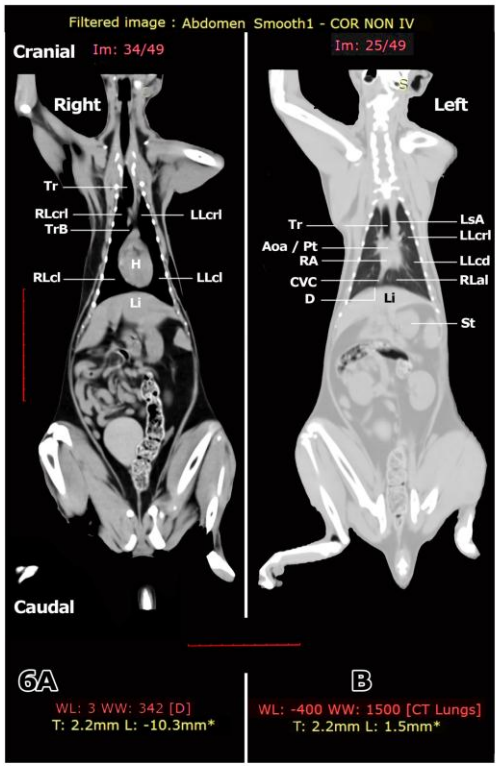

Fig 6: CT windows of coronal slices (6A, soft window; B, lung window) of a healthy 3-year-old Shirazi cat showing the architecture of the lungs with high density. Fig. 6B represented the selected slice No. 25, which was scanned at the level of the middle of the cat i.e., at about the junction of the two halves of the 4 – 10th ribs. Fig. 4A represented the selected slice No. 34, which was scanned ventral to the previous one. Tracheal bifurcation (TrB) was clearly visible dorsal to the base of the heart and left subclavian artery (LsA), which coursed cranial wards left to the trachea. At this level of scanning, three lobes of the right lung were observed; cranial (RLcrl), accessory (RLal) and caudal (RLcl) lobes, meanwhile the two lobes of the left lung were observed; cranial (LLcrl) and caudal (LLcd) lobes. The liver (Li) occupied the intrathoracic part of the abdominal cavity with its major parts located right to the midline, meanwhile the stomach (St) was on the left side (6B). Caudal vena cava (CVC) pierced the diaphragm (D) and coursed between the caudal (RLcl) and accessory (RLal) lobes of the right lung to open into the right atrium (RA).

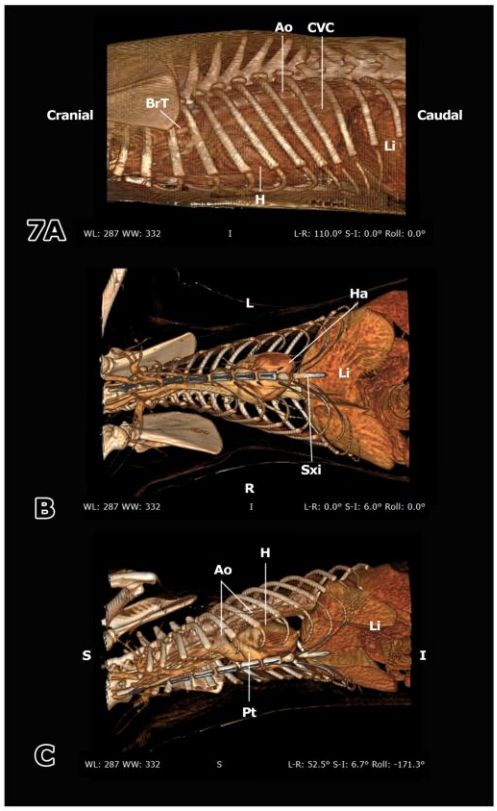

Fig 7: A 3D reconstruction of the thorax of the investigated cats developed by the used CT screening system and showing the thoracic cage and its contents and the relationship between thoracic organs and structures specially the heart, which was easily visualized.